Preparation of 5-benzotriazolyl-4-hydroxy-3-*sec*-butylbenzenesulfonate anion-intercalated layered double hydroxide and its photostabilizing effect on polypropylene

Dianqing Li, Zhenjun Tuo, David G. Evans, Xue Duan*

Key Laboratory of Science and Technology of Controllable Chemical Reactions, Ministry of Education, Beijing University of Chemical Technology, Beijing 100029, China

Abstract

An organic UV absorber has been intercalated into a layered double hydroxide (LDH) host by ion-exchange method using ZnAl–NO₃–LDH as a precursor with an aqueous solution of the sodium salt of 5-benzotriazolyl-4-hydroxy-3-*sec*-butylbenzenesulfonic acid (BZO). After intercalation of the UV absorber, the interlayer distance in the LDHs increases from 0.89 to 2.32 nm. Infrared spectra and thermogravimetry and differential thermal analysis (TG–DTA) curves reveal the presence of a complex system of supramolecular host–guest interactions. The thermostability of BZO is markedly enhanced by intercalation in the LDH host. ZnAl–BZO–LDHs/ polypropylene composite materials exhibit excellent UV photostability.
© 2006 Elsevier Inc. All rights reserved.

Keywords: UV absorber-intercalated LDHs; Benzotriazole; Intercalation; Thermostability; Photostability

1. Introduction

5-Benzotriazolyl-4-hydroxy-3-*sec*-butylbenzenesulfonic acid (abbreviated here as BZO) is an excellent UV absorbing material, which has been used in wool and wood lignin color retention [1]. The molecular structure of BZO is shown in Fig. 1. BZO is a relatively small organic molecule and has poor thermal stability, being readily oxidized at moderate temperatures in air, which restricts its use as a photostabilizer in polymer materials.

Polypropylene (PP) is a widely used general-purpose plastic, but its photostability is poor. UV radiation in sunlight can induce photo-oxidative degradation of PP which has an adverse effect on its mechanical properties. In order to improve the UV resistance of PP, some type of photostabilizer must be added to a PP composite during the manufacturing process.

Layered double hydroxides (LDHs) are a well-known large class of anionic clays [2]. LDHs possess positively charged metal hydroxide layers, which are electrically balanced by the intercalation of anions in the interlayer galleries; these interlayer anions can be replaced by other anions to form a variety of new functional materials [3]. The general formula of LDHs can be represented by $[M_{1-x}^{2+} M_x^{3+}(OH)_2]$ $[A_{x/n}^{n-}.mH_2O]$, where M^{2+} and M^{3+} are metallic cations such as Mg^{2+}, Ni^{2+}, Mn^{2+}, or Zn^{2+} and Al^{3+}, Cr^{3+}, or Fe^{3+}; A^{n-} is an inorganic anion such as CO_3^{2-}, SO_4^{2-}, Cl^-, NO_3^-, or various organic anions; the value x is equal to the molar ratio $M^{3+}/(M^{2+} + M^{3+})$; and m is the number of water molecules located in the interlayer galleries together with the anions. Recently, LDHs have received considerable attention due to their potential applications as catalysts, catalyst supports, electrodes, sensitizers, anionic exchangers, adsorbents, and polymer additives [4–7].

Several examples of the intercalation of organic and inorganic compounds in LDHs have been reported in the literature [2–7]. Perioli et al. have described how the photostability of organic sunscreens may be enhanced by intercalation in LDHs [8,9]. We [10] have successfully intercalated large azo pigment (C.I. Pigment Red 48:2)

*Corresponding author. Fax: +86 10 6442 5385.
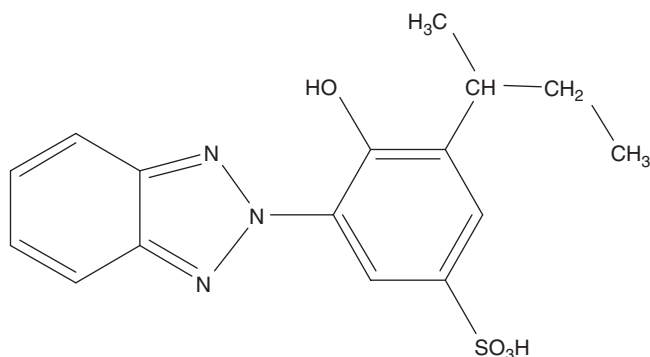E-mail address: duanx@mail.buct.edu.cn (X. Duan).

Fig. 1. Structure of 5-benzotriazolyl-4-hydroxy-3-*sec*-butylbenzenesulfonic acid.

anions into an LDH host by the ion-exchange method. After intercalation, the thermal stability and photostability of the azo pigment anion was found to be markedly enhanced. He et al. [11] reported the intercalation of benzoic acid and benzophenone UV absorbents into LDH hosts, and both the thermal stability and photostability of guest species were improved by intercalation.

In this work, we report the synthesis of BZO anion-intercalated LDHs and the application of the intercalated material as photostabilizer for PP.

2. Experimental section

2.1. Chemicals

$Zn(NO_3)_2 \cdot 6H_2O$, $Al(NO_3)_3 \cdot 9H_2O$, NaOH, and HNO_3 were of A.R. grade, and were purchased from Beijing Chemical Reagent Company. Commercial isotactic PP (1700) was purchased from Yanshan Petrochemical Company. CO_2-free deionized water was used in all experiments and had a conductivity of less than $10^{-6}\,S\,cm^{-1}$. 5-Benzotriazolyl-4-hydroxy-3-*sec*-butyl-benzenesulfonic acid (BZO) was obtained from Ciba Specialty Chemicals Company, and was purified by recrystallization in water.

2.2. Preparation of ZnAl–NO₃–LDH precursor

$Zn(NO_3)_2 \cdot 6H_2O$ (35.7 g, 0.12 mol) and $Al(NO_3)_3.9H_2O$ (22.5 g, 0.06 mol) were dissolved in CO_2-free deionized water (150 mL) to make a mixed salt solution. NaOH (14.4 g, 0.36 mol) was dissolved in CO_2-free deionized water (150 mL) to make an alkali solution. These two solutions were simultaneously added to a colloid mill [12] with rotor speed set at about 4000 rpm and mixed for 2 min. The resulting slurry was transferred into a four-neck flask as quickly as possible and aged at 100 °C for 6 h in a flowing N_2 stream. After centrifugation and extensive washing, a portion of the precipitate was dried at 70 °C for 24 h, giving the precursor ZnAl–NO₃–LDHs.

2.3. Assembly of BZO anion-intercalated LDHs

BZO anion-intercalated LDH (ZnAl–BZO–LDHs) was prepared by an anion-exchange method using ZnAl–NO₃–LDH as precursor. An amount of the above slurry of ZnAl–NO₃–LDHs containing about 3.45 g (ca. 0.01 mol of NO_3^-) of dry solid was dispersed in CO_2-free deionized water (150 mL). BZO (5.2 g, 0.015 mol) was dissolved in CO_2-free deionized water (150 mL) and the pH value of the solution was adjusted to around 7 by adding NaOH. The BZO solution was added dropwise to the LDH suspension (the final molar ratio of BZO/NO₃ was 1.5, i.e. BZO was present in excess of the theoretical exchange capacity) and the mixture subsequently aged at 100 °C under N_2 protection for about 6 h. The final pH of the solution was 6.8. The resulting precipitate was centrifuged, thoroughly washed, and dried at 70 °C overnight and stored in a sample bottle under nitrogen.

2.4. Photostabilization testing of ZnAl–BZO–LDHs/PP composite

ZnAl–BZO–LDH (1.0 wt%) was thoroughly mixed with PP powder in a double roller mixer at 160 °C for 10–20 min and molded into a composite film (30 × 30 × 0.05 mm) after heating at 180 °C. The time of molding was 3 min. A composite containing PP and pristine BZO could not be obtained under the same conditions due to the poor thermal stability of BZO, which appeared charred and black at this temperature. The ZnAl–BZO–LDHs/PP composite and pristine PP films were exposed to a UV lamp (wavelength range: 250–380 nm, 1000 W) in a UV-aging test box. The distance between samples and ultraviolet light source was 15 cm. The maximum temperature of the sample surface during irradiation was 70 °C.

2.5. Analysis and characterization

Powder X-ray diffraction (XRD) measurements were performed on Shimadzu XRD-6000 X-ray powder diffractometer (Cu$K\alpha$ radiation, $\lambda = 0.15406$ nm) between 3° and 70°. The scan speed was $5°\,min^{-1}$. Infrared (IR) spectra were recorded on a Bruker Vector 22 Fourier-transform IR spectrophotometer using the KBr disk method with a ratio of sample/KBr of 1:100 by mass. Thermogravimetry and differential thermal analysis (TG–DTA) curves were obtained on a Beifen PCT-IA instrument in the temperature range 40–600 °C with a heating rate of $10\,°C\,min^{-1}$ in air. The particle-size distribution was determined with a Malvern Mastersizer 2000 laser particle-size analyzer. Elemental analysis (Zn, Al, S) was carried out using a Shimadzu ICPS-7500 Inductively Coupled Plasma (ICP) Emission Spectrometer. Diffuse reflectance UV–visible absorbance spectra were recorded using a Shimadzu UV-2501PC instrument with an integrating sphere attachment in the range 200–800 nm

Table 1
Composition of ZnAl–NO$_3$–LDHs and ZnAl–BZO–LDHs

Sample	Zn (wt)%	Al (wt)%	S (wt)%	Zn/Al molar ratio	Formula
ZnAl–NO$_3$–LDHs	35.9	7.45	—	1.99	Zn$_{0.66}$Al$_{0.34}$(OH)$_2$(NO$_3$)$_{0.33}$ · 0.75H$_2$O
ZnAl–BZO–LDHs	18.52	5.13	6.14	2.00	Zn$_{0.66}$Al$_{0..33}$(OH)$_2$(C$_{16}$H$_{17}$N$_3$O$_4$S)$_{0.33}$ · 1.08H$_2$O

using BaSO$_4$ as reference. UV-irradiated samples were analyzed immediately after exposure.

3. Results and discussion

3.1. Elemental analysis

The results of elemental analysis and the calculated stoichiometries of the LDH precursor and BZO intercalate are given in Table 1. The quantities of water were estimated from the TG data. The results confirm that BZO anions have replaced the original NO$_3^-$ anions and that the intercalation process has no influence on the composition of LDH layers, with the Zn/Al ratio remaining essentially unchanged.

3.2. XRD patterns of the samples

The ZnAl–NO$_3$–LDH precursor was prepared by a method involving separate nucleation and aging steps developed in our laboratory [12,13]. In order to maximize the charge density of the layers and hence the amount of intercalated guest, a Zn/Al molar ratio of 2 was employed. XRD patterns of ZnAl–NO$_3$–LDH and ZnAl–BZO–LDH are shown in Fig. 2. The XRD pattern of the ZnAl–NO$_3$–LDH precursor exhibits typical characteristics of an LDH (hydrotalcite-like) phase. The sharp, symmetrical peaks at low angle correspond to the basal and higher order reflections. The basal spacing (d_{003}) of the ZnAl–NO$_3$–LDH sample is 0.89 nm. After the ion-exchange reaction, the basal spacing was expanded to 2.32 nm indicating that BZO anions have been intercalated into the interlayer galleries of LDH precursor because the size of BZO anions is larger than that of NO$_3^-$ groups. The weak (110) reflections at $2\theta \sim 61°$ show little change on intercalation. Since the value of $2(d_{110})$ represents the distance between two adjacent metallic cations in the lattice [14], this indicates that the metal hydroxide layers have not been destroyed by BZO during ion-exchange reaction.

3.3. Host–guest interactions

Fig. 3 shows the FT-IR spectra of ZnAl–NO$_3$–LDHs, BZO, and ZnAl–BZO–LDHs. The spectrum of ZnAl–NO$_3$–LDH (Fig. 3a) shows the strong broad absorption band at around 3500 cm^{-1} which can be attributed to the O–H stretching vibration of hydroxyl groups in the brucite-like layers and water in the galleries [15]. The sharp band at around 1384 cm^{-1} corresponds to the v_3 stretching vibra-
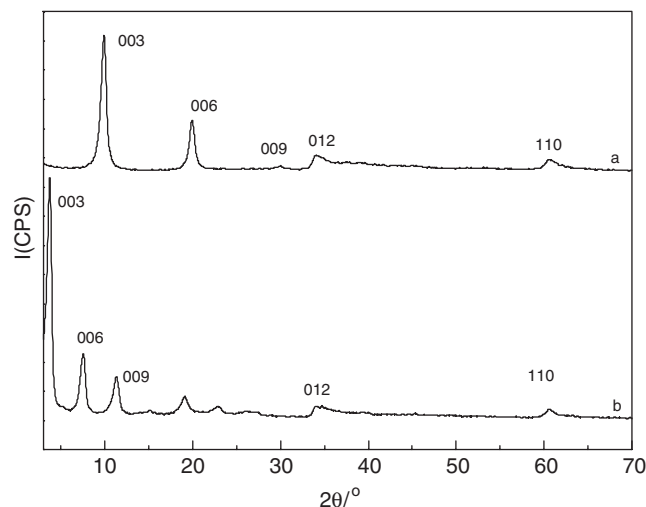
Fig. 2. XRD patterns of (a) ZnAl–NO$_3$–LDH precursor and (b) ZnAl–BZO–LDHs.
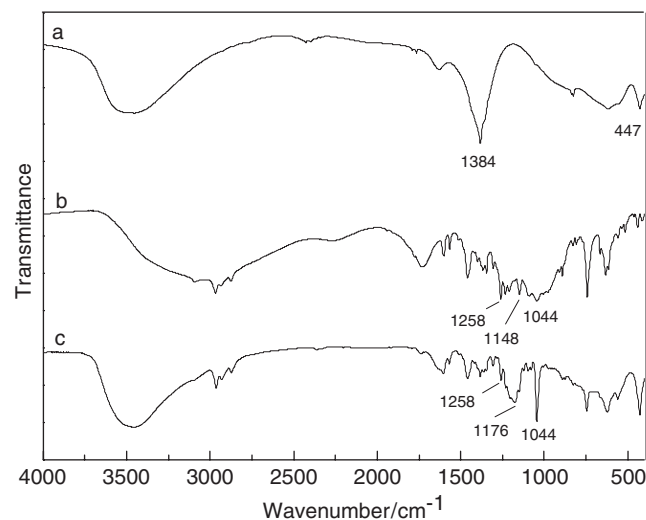
Fig. 3. FT-IR spectra of (a) ZnAl–NO$_3$–LDHs, (b) BZO and (c) ZnAl–BZO–LDHs.

tion of NO$_3^-$ groups [15]. In the lower wavenumber range, the band at 447 cm^{-1} can be ascribed to O–M–O vibrations in the brucite-like layers of the LDH [15]. The FT-IR spectrum of BZO (Fig. 3b) shows strong absorption bands at 1044, 1148, and 1258 cm^{-1}, which can be attributed [15] to C–S–O, S–O–H, and O=S=O vibrations of the sulfonate group, respectively. After intercalation (Fig. 3c), the NO$_3^-$ absorption band is lost, consistent with the

complete replacement of NO_3^- groups by BZO anions. The band at $1148\,cm^{-1}$ in BZO is shifted to higher frequency in the intercalated material and is located at $1176\,cm^{-1}$. This is indicative of the formation of hydrogen bonds between SO_3^- groups and the hydroxide layers [15].

The TG–DTA curves of the BZO and ZnAl–BZO–LDH are shown in Fig. 4. The decomposition of BZO (Fig. 4a) shows a multi-step weight loss from 40 to 600 °C. Onset of weight loss occurs at around 100 °C, with a rapid weight loss in the temperature range 230–340 °C. However, the DTA curve shows only a broad weak exothermic peak in this temperature range. This is probably a result of the exothermic peak corresponding to partial combustion of BZO being overlapped by an endothermic peak associated with BZO decomposition. The remaining organic species undergo combustion at around 550 °C, with an associated exothermic peak. After intercalation, the shape of the TG curve (Fig. 4b) is quite different from those of the BZO. The first and second weight loss stages below 300 °C correspond to the liberation of physisorbed and chemisorbed water. Two exothermic peaks can be seen between 420 and 480 °C, which correlate with the combustion of the organic materials.

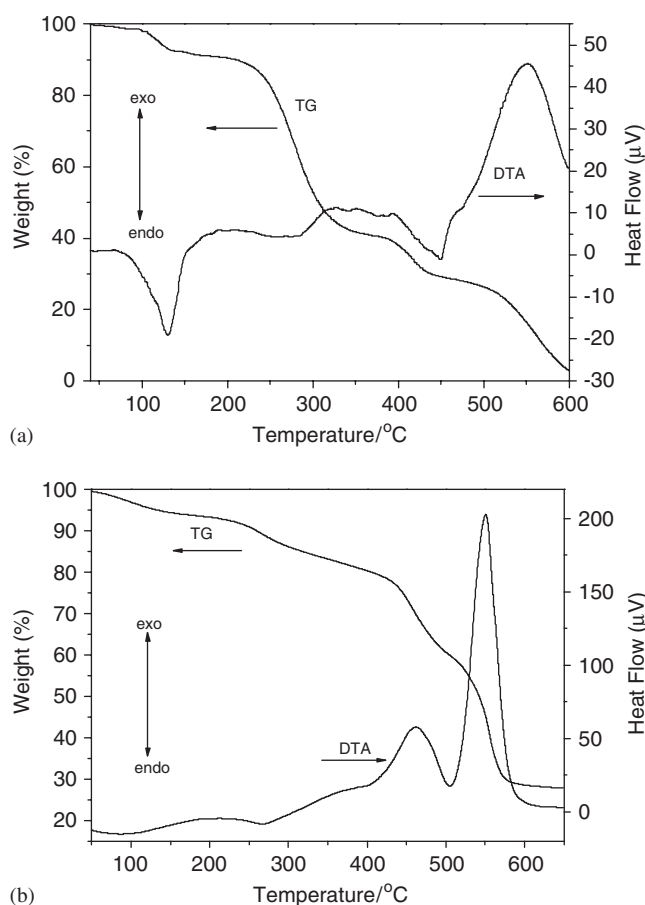From the differences between the IR spectra and TG–DTA curves of free and intercalated BZO, it can be inferred that the intercalation process has given rise to a complex system of strong supramolecular interactions between host layers and guests.

3.4. UV screening capability

Fig. 5 shows the UV transmittance curves of ZnAl–NO_3–LDHs, BZO, and ZnAl–BZO–LDHs. ZnAl–NO_3–LDH have strong UV absorption bands at around 300 and 230 nm (Fig. 5a), which are associated with the presence of NO_3^- groups in the interlayer galleries [16]. These peaks disappear after intercalation however (Fig. 5c), consistent with complete exchange of NO_3^- by BZO anions. The UV transmittance curve of BZO, shown in Fig. 5b, indicates that BZO has strong UV absorption below 400 nm. After intercalation, the UV absorbent-intercalated LDHs exhibit excellent UV absorption ability, comparable to BZO itself below 400 nm (Fig. 5c). As shown in Fig. 6, the particle-size distributions
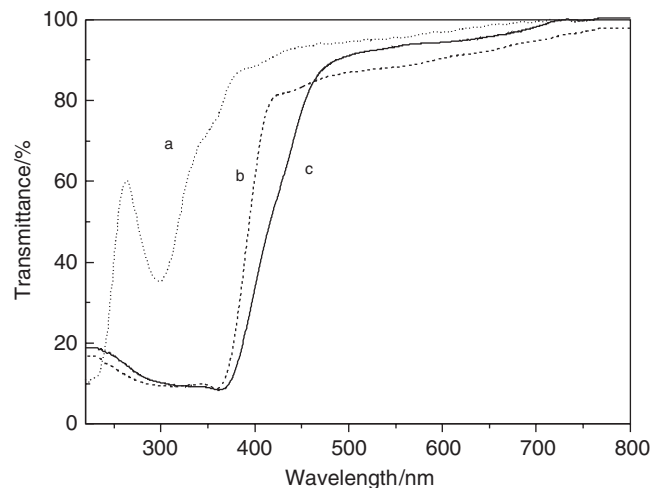
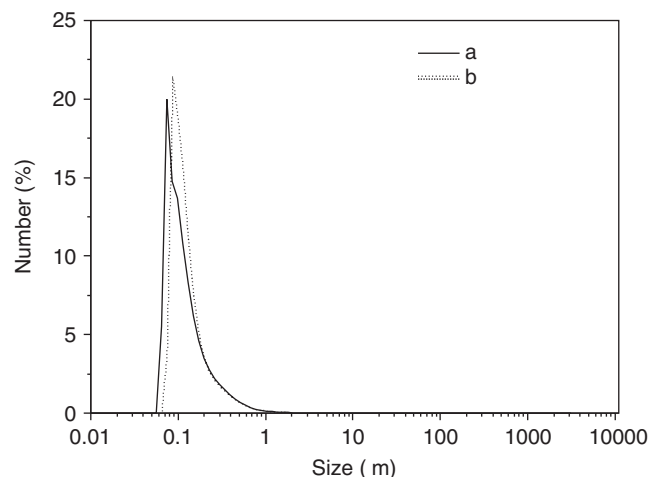Fig. 5. UV transmittance curves of (a) ZnAl–NO_3–LDHs, (b) BZO and (c) ZnAl–BZO–LDHs.

Fig. 4. TG–DTA curves of (a) BZO and (b) ZnAl–BZO–LDHs.

Fig. 6. Particle-size distribution of ZnAl–NO_3–LDH and ZnAl–BZO–LDHs.

of ZnAl–NO$_3$–LDHs and ZnAl–BZO–LDHs are similar indicating that intercalation is not accompanied by a significant change in particle size. This is confirmed by comparing the linewidths in the XRD diffraction patterns. These indicate that the sizes of the platelet-like crystallites in both a and c directions do not change significantly after intercalation of BZO.

From the above analysis of the UV–visible spectra, XRD, IR, and TG–DTA data, it can be inferred that ZnAl–BZO–LDH does not have to behave as a physical mixture of UV absorbent and LDHs, but rather as a complex composite, which possesses superior thermal stability and high UV absorbency.

3.5. Photostabilization of PP by addition of ZnAl–BZO–LDHs

The photo-oxidative degradation mechanism of PP has been widely studied [17–19]. Commercial PP, similar to other polyolefins, contains small amounts of catalyst residues and unsaturated (vinyl or vinylidene) groups as well as carbonyl and hydroperoxide groups, of which the latter play the role of photoinitiator. Their excitation and cleavage with the formation of free radicals is the primary process, followed by chain degradation producing more and more hydroperoxide and carbonyl groups.

The formation and disappearance of functional groups on a PP film surface during photodegradation were monitored by reflectance IR spectroscopy. The FT-IR spectra of pristine PP and ZnAl–BZO–LDHs/PP (Fig. 7) were characterized by bands at the following wavenumbers (cm^{-1}): 1456 (–CH$_3$ asymmetric deformation), 1376 (–CH$_3$ symmetric deformation), 1165 (bending vibration of tertiary carbon), 974, 841, and 808 cm^{-1} (C–H out-of-plane deformations) [18]. A weak peak at 1744 cm^{-1} in the spectrum of PP indicates the presence of carbonyl impurities. After exposure to UV light for 35 min, carbonyl peaks at 1730 cm^{-1} [19] were clearly apparent in the spectra of both pristine and modified PP, and the intensity of the hydroxyl peaks (3000–3600 cm^{-1}) increased. An internal standard method was adopted to compare the behavior of pristine and modified PP. The peak at 841 nm (C–H out-of-plane deformation), the intensity of which is invariant
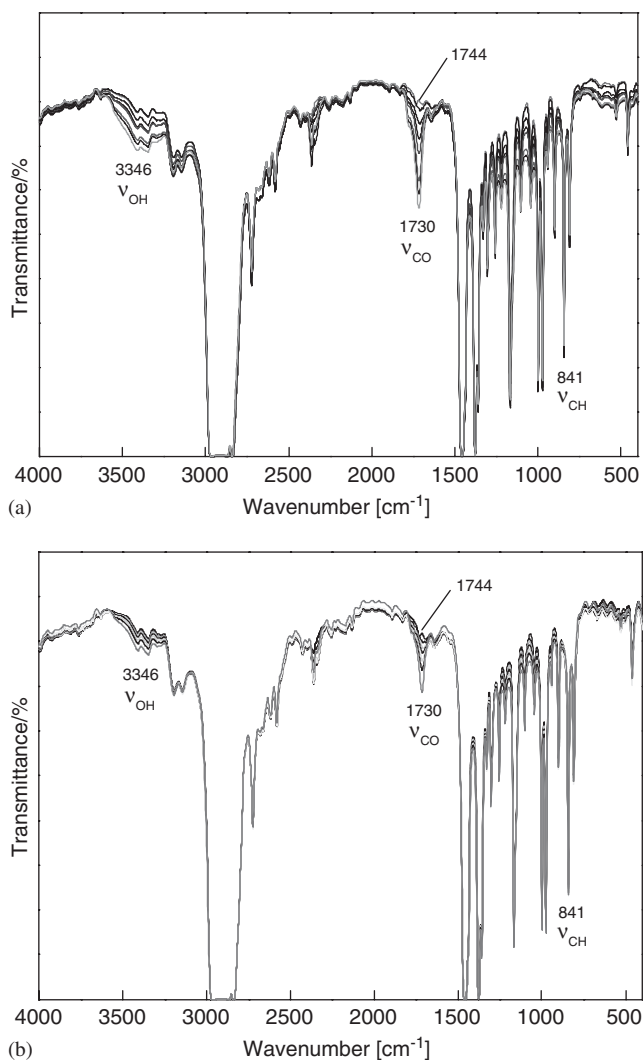

Fig. 7. FT-IR spectra of (a) pristine PP and (b) PP modified by 1% ZnAl–BZO–LDHs.
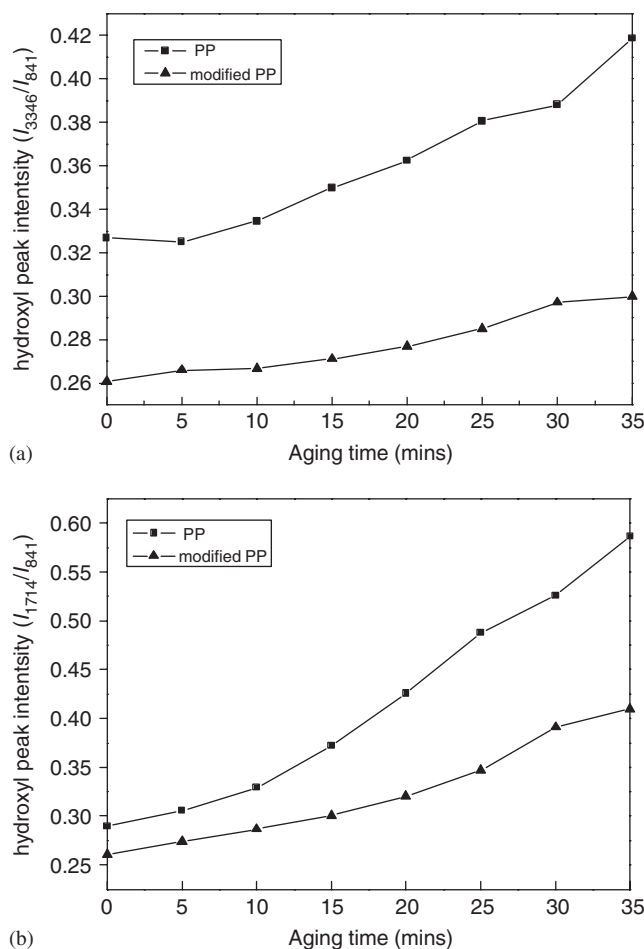

Fig. 8. Variation with UV exposure time of relative peak intensities of (a) hydroxyl and (b) carbonyl bands for pristine PP and PP modified by 1% ZnAl–BZO–LDHs.
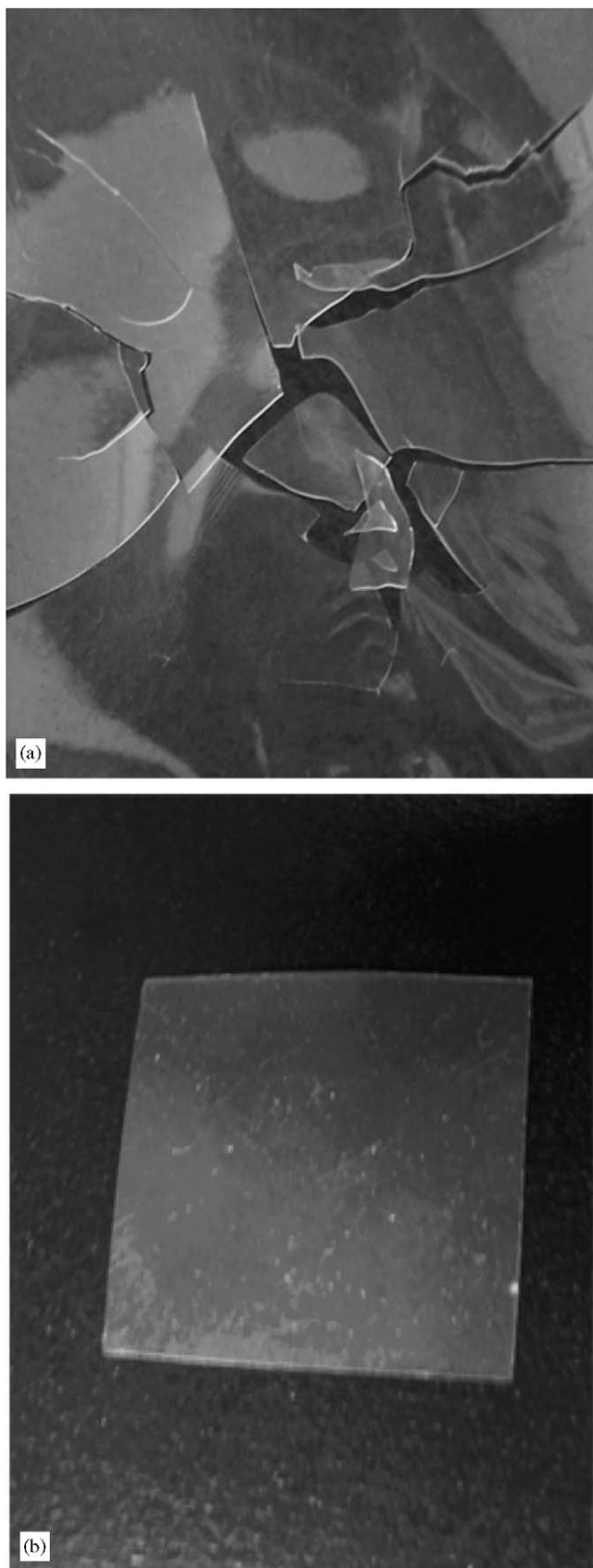
Fig. 9. Photographs of pristine PP (a) and modified PP (b) after UV exposure for 15 min.

under UV irradiation, was chosen as the standard peak, and the absorption intensity ratios I(carbonyl)/I(C–H) and I(hydroxyl)/I(C–H) were calculated. The results, as shown in Fig. 8, clearly indicate that the rate of formation of C=O and OH/OOH groups under UV irradiation is significantly lower in ZnAl–BZO–LDHs/PP than in pristine PP. It is clear therefore that addition of ZnAl–BZO–LDH markedly enhances the photostability of PP.

Furthermore, as shown in Fig. 9, it was found that the pristine PP specimen becomes brittle after exposure to UV light, whilst under the same conditions the modified PP retained good mechanical properties.

4. Conclusions

An anionic UV absorbent has been intercalated into an LDH host by ion exchange of an LDH nitrate precursor with an aqueous solution of the UV absorbent, 5-benzotriazolyl-4-hydroxy-3-*sec*-butylbenzene sulfonic acid. After intercalation of the UV absorbent, the interlayer distance of the hybrid LDHs increases to 2.32 nm while the basal spacing of precursor LDHs is only 0.89 nm. Elemental analysis and TG data show that the material has the composition $Zn_{0.66}Al_{0.33}(OH)_2(C_{16}H_{17}N_3O_4S)_{0.33} \cdot 1.08H_2O$. Analysis of FT-IR spectra indicated that there is a complex system of supramolecular interactions between the host layers and guest anions in the intercalated structure. The UV absorption ability of the BZO-intercalated LDHs is as high as that of the pure UV absorbent but the former shows much better thermostability than the latter. Onset of decomposition of BZO is observed at 250 °C, whilst that the UV absorbent intercalated LDH is stable below 450 °C. When the BZO-intercalated LDH was incorporated in a PP composite, the photostability of the resulting film was also markedly enhanced compared to that of the pristine PP.

Acknowledgment

References

[1] P. McGarrya, C. Heitner, J. Schmidt, A. Rodenheiser, R. St. John Manley, G. Cunkle, T. Thompson, J. Photochem. Photobiol. A: Chem. 151 (2002) 145.

[2] V. Rives (Ed.), Layered Double Hydroxides: Present and Future, Nova Science Publishers, New York, 2001.

[3] F. Cavani, F. Trifiro, A. Vaccari, Catal. Today 11 (1991) 173.

[4] P.S. Braterman, Z.P. Xu, F. Yarberry, in: S.M. Auerbach, K.A. Carrado, P.K. Dutta (Eds.), Handbook of Layered Materials, Marcel Dekker, New York, 2004, pp. 373–474 (Chapter 8).

[5] F. Leroux, C. Taviot-Gueho, J. Mater. Chem. 15 (2005) 3628.

[6] D.G. Evans, X. Duan, Chem. Commun. (2006) 485.

[7] F. Li, X. Duan, Struct. Bond. 119 (2006) 193.

[8] L. Perioli, V. Ambrogi, B. Bertini, M. Ricci, M. Nocchetti, L. Latterini, C. Rossi, Eur. J. Pharm. Biopharm. 62 (2006) 185.

 [9] L. Perioli, V. Ambrogi, C. Rossi, L. Latterini, M. Nocchetti, U. Costantino, J. Phys. Chem. Solids 67 (2006) 1079.

[10] S. Guo, D. Li, W. Zhang, M. Pu, D.G. Evans, X. Duan, J. Solid State Chem. 177 (2004) 4597.

[11] Q. He, S. Yin, T. Sato, J. Phys. Chem. Solids 65 (2004) 395.

[12] Y. Zhao, F. Li, R. Zhang, D.G. Evans, X. Duan, Chem. Mater. 14 (2002) 4286.

[13] X. Duan, Q. Jiao, L. Li, Chn. Pat., 1999, CN99119385.7.

[14] V. Rives, Mater. Chem. Phys. 75 (2002) 19.

[15] J. Wang, M. Wei, J. He, D.G. Evans, X. Duan, J. Solid State Chem. 177 (2004) 366.

[16] J. Mack, J.R. Bolton, J. Photochem. Photobiol. A: Chem. 128 (1999) 1.

[17] D. Ramkumar, M. Bhattacharya, U. Vaidya, Eur. Polym. J. 33 (1997) 729.

[18] P. He, Y. Xiao, P. Zhang, C. Xing, N. Zhu, X. Zhu, D. Yan, Polym. Degr. Stab. 88 (2005) 473.

[19] Z. Dong, Z. Liu, B. Han, J. He, T. Jiang, G. Yang, J. Mater. Chem. 12 (2002) 3565.